Available online at www.sciencedirect.com
ScienceDirect
Computers and Geotechnics 33 (2006) 209–221
COMPUTERS AND GEOTECHNICS
www.elsevier.com/locate/compgeo

Working mechanism of cutoff walls in reducing uplift of large underground structures induced by soil liquefaction

Huabei Liu *, Erxiang Song

Department of Civil Engineering, Tsinghua University, Haidian District, Beijing 100084, PR China

Received 23 April 2006; received in revised form 3 July 2006; accepted 4 July 2006
Available online 8 August 2006

Abstract

The uplift of large underground structures in saturated liquefiable soils under strong earthquake loadings may induce severe damages to the structures. Various mitigation procedures have been proposed to alleviate such damage, among which installation of cutoff walls next to underground structures was found to be effective. However, the working mechanism of cutoff walls in alleviating uplift of underground structures and the corresponding design parameters are still not clear. The liquefaction induced uplift behaviour of a subway tunnel in saturated sandy deposit over a layer of non-liquefiable soils and the working mechanism of cutoff walls for uplift mitigation purpose were investigated using the fully coupled dynamic finite element code DIANA Swandyne-II. A generalized plasticity model capable of simulating both cyclic liquefaction and pressure dependency of soils was used to model the sandy deposit. It is found that the small effective unit weight of underground structures, the development of excess pore pressure and the flow of liquefied soils were the sufficient and necessary conditions for underground structures to uplift during earthquakes. Cutoff walls could restrain the flow or deformation of liquefied soils and inhibit the uplift of underground structures but they could not necessarily prevent the liquefaction of the enclosed soils. After earthquake loadings, underground structures might settle due to the consolidation of soils and cutoff walls could also reduce the magnitude of settlement. The design parameters of cutoff walls, including the acting lateral pressure, the position, the stiffness and the permeability of cutoff walls, were also analyzed, the findings of which, together with the unveiled working mechanism, would be relevant for the design of cutoff walls for uplift mitigation purpose.

Keywords: Large underground structure; Earthquake; Liquefaction; Uplift; Cutoff walls; Mechanism; Design parameters

1. Introduction

Underground structures in saturated liquefiable soils may be subjected to severe damages during earthquake. One of the reasons is the uplift or even floatation of underground structures due to soil liquefaction. Subway tunnels or underground pipelines, for example, may be subjected to very large shear load if part of the tunnels or pipelines are in liquefiable soils and prone to uplift while the other in non-liquefiable ones. The shear load may be much larger than the shear strength of the underground structures. The soil liquefaction induced uplift of underground pipelines during strong earthquake was observed as early as in 1964 Niigata Earthquake and Alaska Earthquake [1]. Such damages were found in many recent large earthquakes, such as 1989 Loma Priesta Earthquake [2], 1993 Hokkaido–Nansei–Oki Earthquake [3], 1994 Hokkaido–Toho–Oki Earthquake [4], 1995 Kobe Earthquake [5] and 1999 Taiwan Earthquake [6]. Liquefaction induced uplift of large underground structures can also be found. It was reported that some tunnels were prone to floatation during the 1989 Loma Priesta Earthquake [7].

Different mitigation strategies have been proposed to eliminate or alleviate uplift damages, which includes densification or replacement of the surrounding liquefiable soils [8], installation of gravel drainage [8,9], grouting [10] and installation of cutoff walls [11–14]. Soil replacement may

* Corresponding author. Tel.: +86 10 62785681; fax: +86 10 62771132.
E-mail address: lhb@tsinghua.edu.cn (H. Liu).

0266-352X/$ - see front matter © 2006 Elsevier Ltd. All rights reserved.
doi:10.1016/j.compgeo.2006.07.002

be too expensive if the liquefiable soil layer is too thick. Gravel drainage was found to be a very effective countermeasure again the uplift of small underground structures [9]. It is also possible to be used for large underground structures constructed using cut-and-cover method, although it may have to be carefully designed and combined with other mitigation procedures [8], since the drainage path in most cases of large underground structures may be too long and the dissipation of excess pore pressure would not be quick enough to prevent uplift. But it is difficult for underground structures constructed using tunneling methods. The method of grouting may be useful as well [10], but it is also too expensive for thick liquefiable soil layers. Comparatively, the installation of cutoff walls could be effective and much economical. Cutoff walls can be constructed using different kinds of methods and materials [11–14], and additional drainage paths can be provided by cutoff walls if materials with high permeability are used (e.g. [11]). The installation of cutoff walls for uplift alleviation is illustrated in Fig. 1. In order that cutoff walls can be effective, they must be sufficiently extended into the underlying non-liquefiable soils [12–14].

However, the working mechanism of cutoff walls is still not clear and the corresponding design parameters also need to be investigated in depth. The working mechanism of cutoff walls is directly related to the uplift mechanism of underground structures in liquefiable soils. It is already found that the small effective unit weight of underground structures and the development of excess pore pressure are two necessary conditions for underground structures to uplift during earthquake [7]. However, they are not sufficient conditions. The liquefiable soil must be allowed to flow or deformed and "squeeze" beneath underground structures so that they would be "pushed up". Such mechanism was discussed in [12,13,15] but no direct evidences have ever been reported.

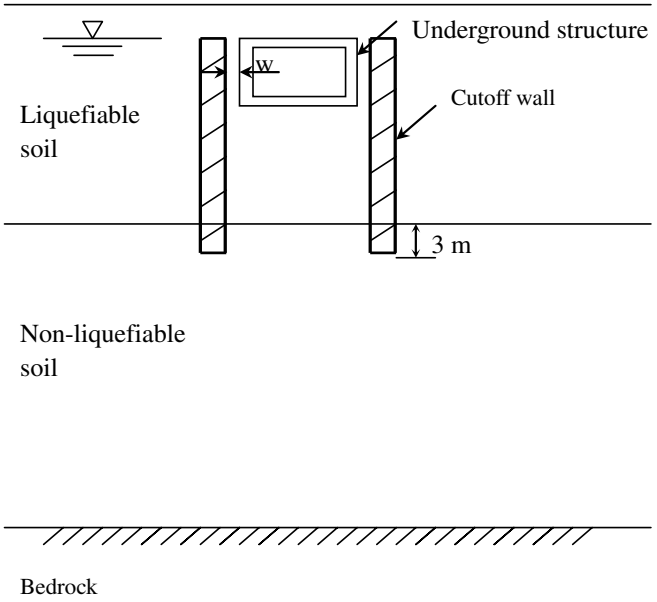

Fig. 1. Illustration of cutoff walls.

The installation of cutoff walls can prevent the flow or deformation of liquefiable soils and hence alleviate uplifting of underground structures. However, it was also reported that cutoff walls were able to reduce the development of excess pore pressure underneath underground structures [14]. The conclusion was based on the shaking table tests on underground structures buried in very loose saturated sand ($Dr = 15\%$ Toyoura sand). Cutoff walls have also been proposed to alleviate the settlement of surface structures on liquefiable soils [16,17]. The findings of these investigations [16,17] were contradictory to each other. In Zheng et al. [16], cutoff walls were found to be able to reduce the excess pore pressure build-up while subjected to small earthquake excitation; but in Adalier et al. [17], the excess pore pressure in the soils enclosed by cutoff walls was found to be no smaller than that in the case without cutoff walls.

The working mechanism of cutoff walls in alleviating uplift of underground structures must be clearly understood so that their rational design can be conducted. In order to achieve this purpose, model testing would be direct and helpful, while verified numerical procedures could also be effective. Comparatively, more useful results may be obtained using numerical methods and the mechanism of uplift of underground structures and the working mechanism of cutoff walls can be scrutinized more closely. The design parameters of cutoff walls can also be investigated in depth with numerical methods. Verified numerical procedures like finite element method have been successfully used to analyze the responses of underground structures in liquefiable soils [10,18,19]. In Liu and Song [10], a 2-D, effective-stress-based, fully coupled, finite element code DIANA Swandye-II [20] was used to analyze the seismic responses of large underground structures in liquefiable soils subjected to horizontal and vertical earthquake excitations. The finite element code used in that study has been frequently used to analyze soil–structure interaction problems involving soil liquefaction (e.g. [21,22]). A generalized plasticity model that can simulate the pressure dependency and cyclic hardening properties of sand [23,24] was incorporated into the program by the first author [25] and used to conduct the analyses in Liu and Song [10].

In this study, the finite element procedure that is similar to that in Liu and Song [10] was used to investigate in depth the uplift mechanism of large underground structures in liquefiable soils and the working mechanism of cutoff walls in alleviating uplift. The investigation focused on the uplift behaviour of underground structures and the in-plane seismic induced stresses were not discussed. A simple rectangular subway tunnel was used in the study, which was assumed to be constructed in a layer of saturated loose sandy soil over a layer of stiff non-liquefiable soil. The cutoff walls were assumed to be constructed using grouting method, but different coefficients of permeability were

analyzed to inspect the effects of drainage. Horizontal earthquake record from the 1995 Kobe Earthquake was used as input excitation. The behaviour of the soil–structure system after earthquake was also investigated and the parameters that are needed in the design of cutoff walls were discussed, especially the lateral pressures acting on the cutoff walls.

2. Finite element model

2.1. Physical model

The uplift behaviour of a subway tunnel subjected to earthquake induced liquefaction in a model ground was investigated. The subway tunnel was assumed to be rectangular, with a width of 10 m and a height of 5 m, buried in loose saturated sand at a depth of 3 m. The thickness of the saturated sand layer was assumed to be 20 m, with a 21-meter-thick layer of stiff non-liquefiable soil beneath it, which again lay on the bedrock. The thickness of the walls, the boards and the columns of the subway tunnel were all assumed to be 0.6 m. Cutoff walls, if installed, were extended into the non-liquefiable soils for 3 m and enclosed the subway tunnel and the soils underneath it, as illustrated in Fig. 1. However, the thickness, the modulus, and the horizontal locations of the cutoff walls were varied in the analyses to investigate the designing parameters. Plane strain condition was assumed in the finite element models.

2.2. Material modeling and properties

The constitutive models and material properties as used in Liu and Song [10] were used in the present study. The liquefiable sandy soil was assumed to be isotropic and simulated using a non-associated generalized plasticity model that is capable of modeling cyclic liquefaction, cyclic hardening and pressure dependency of sandy soil. The behaviour of sands under monotonic and cyclic loadings at different mean effective stress levels can be reproduced using the model. The description of the model can be found in other publications [10,23–25] and is not undertaken herein. The parameters for the loose Nevada sand ($Dr = 40\%$) used in Liu and Song [10] were also used in this study, as shown in Table 1. The model parameters were calibrated using monotonic and triaxial test results [26] and used to simulate one of the centrifuge shaking table tests on sandy deposit in the VELACS project (Test 2 of Model No. 1 conducted at RPI) [27]. The sand deposit was 20 cm thick, saturated with water, and was subject to 20-cycle sinusoidal wave of 11.75 g at 100 Hz with a centrifugal force of 50 g. The simulated acceleration and excess pore pressure in the soil deposit were compared to the experimental ones and they were found to agree well with each other. The excess pore pressure dissipation after shaking was also simulated and the results were good. The details of the simulation can be found in Yang and Ling [28]. The simulation results indicate that although with isotropy assumption, the generalized plasticity model in Ling and Liu [24] could be used to simulate earthquake induced liquefaction of sandy soil.

The coefficient of permeability and the void ratio of the loose sandy soil were 6.6×10^{-2} cm/s and 0.74, respectively. The permeability of the liquefiable soil was raised 10 times larger in purpose in comparison to the real coefficient of loose Nevada sand [26] so that the consolidation analysis after earthquake excitation would not be very long. It must be pointed out that the increase of permeability influences only very slightly the seismic behaviour of the soil–structure system during earthquake excitation, according to the trial analyses by the authors. A 5% viscous

Table 1
Material parameters

Loose sandy soil		Interface		Subway tunnel		Stiff soil layer	
Shear modulus G (Pa)	250	Young's modulus E (kPa)	5000	Young's modulus (MPa)	30,000	G_0 (MPa)	11.4
Bulk modulus K (Pa)	300	Tangent modulus G (kPa)	1000	Poisson's ratio	0.2	K_0 (MPa)	24.7
φ_0 (°)	38	Friction angle δ (°)	23	Unit weight (kN/m^3)	24	p_0 (kPa)	100
$\Delta\varphi$ (°)	0.25	Cohesion c (kPa)	0			Dry unit weight (kN/m^3)	16.4
M_g	1.25	Tension strength (kPa)	0				
M_f	1.18						
α	0.45						
β_{10}	2.8						
β_0	9.0						
H_0 (Pa)	200						
H_{u0} (Pa)	400						
r	1.0						
r_u	3.5						
r_d	80						
k_s	0.01						
Dry unit weight (kN/m^3)	15.0						
Coefficient of permeability (cm/s)	6.6×10^{-2}						

damping of Rayleigh type was included in the dynamic analyses apart from the inherent hysteresis damping of the constitutive model [10,25].

The non-liquefiable soil was simulated using the General-Power-Elastic-One model available in DIANA Swandyn-II, which is able to describe the dependency of soil stiffness on confining pressure. The shear and bulk moduli of the non-liquefiable soil were defined as

$$G = G_0(p'/p_0)^{0.5}, \quad K = K_0(p'/p_0)^{0.5} \tag{1}$$

in which p_0 is the reference pressure while p' is the present mean effective stress. G_0 and K_0 are the shear and bulk moduli at the reference pressure level, respectively. The model parameters for the non-liquefiable soil are shown in Table 1, which were obtained by referring to the normal stiffness of stiff soils. The dry unit weight (γ_d) of the non-liquefiable soil was assume to be 16.4 kN/m^3, and its coefficient of permeability was assumed to be the same as that of the liquefiable soil. A 5% viscous damping of Rayleigh type was used for the non-liquefiable soil in the analyses. The authors are aware that the elastic and damping properties of the non-liquefiable soil would influence the magnitude of the seismic response; however, they would not affect the conclusions that the present study tried to obtain.

The subway tunnel was assumed to be linear elastic, modeled using Mindlin beam elements. Typical elastic properties of concrete were assigned to it, as shown in Table 1. The unit weight of the reinforced concrete was taken as 24 kN/m^3. A 5% viscous damping of Rayleigh type was also used for the subway tunnel.

The interface between the soil and the subway tunnel was modeled using thin-layer quadrilateral isoparametric elements, the thickness-length ratio of which was about 1–20 to 1–10. The constitutive properties of the interface were simulated using the SLIP ELEMENT III model available in the finite element code. The slippage of the interface was governed by the Mohr–Coulomb friction criterion, and before slippage, the interface behaved elastically, with uncoupled normal and tangential stiffness. The normal stiffness was calculated from the Young's modulus, while the tangential stiffness could be obtained from the "tangent" modulus, as shown in Table 1. Cutoff tension could be defined to simulate the separation of interface. The unloading and reloading behaviours were assumed to be linear elastic, and possible shear dilation of the interface as well as the drainage path provided by the interface was not considered in the finite element model. The friction angle of the interface was obtained using $\delta = \tan^{-1}[(2/3)\tan\varphi]$, in which $\varphi = 32°$ is the angle of internal friction of the liquefiable soil. The model parameters for the interface are shown in Table 1. Small "tangent" modulus was used for the interface in order to simulate its behaviour in relatively large deformation [10,21]. The authors understand the fact that soil–structure interface behaviour can be much more complicated than what the SLIP ELEMENT model can describe, but it is able to simulate the most important features of interface, including slippage, separation and closure.

The cutoff walls were assumed to be constructed using injection grouting, which were assumed to be linear elastic with a Young's modulus of 400 MPa for the base case and varied in the parametric study. The Poisson's ratio was 0.25. The coefficient of permeability of the cutoff walls was assumed to be 6.6×10^{-6} cm/s, unless otherwise stated for the purpose of investigating the effect of drainage. The cutoff walls and the liquefiable soils were assumed to be perfectly bonded, i.e., no interface elements were used between them. The assumption was based on the fact that the interaction between them was not important for the uplift response of the subway tunnel and it could considerably reduce the complexity of the finite element models.

2.3. Finite element mesh and boundary conditions

The finite element mesh is shown in Fig. 2. Altogether 2241 elements and 9155 nodes were used. Among the elements, 2184 were two-phase, eight-node, quadrilateral elements for the saturated soils and/or the cutoff walls; 26 were eight-node thin-layer slip elements; and 31 were 3-noded Mindlin beam elements. The finite element meshes for the cases with and without cutoff walls were kept the same to eliminate mesh effects.

The boundary between the soil deposit and the bedrock was assumed to be fixed. The ground surface was assumed to be flat and free of loadings and the underground water level was assumed to locate at the ground surface. The tied node feature of the finite element code [20] was used for the side boundaries, the horizontal and vertical displacements at which were restrained to have the same value, and a relatively large analyzed domain (198 m) was used, in order to simulate the free field response in the far field of the subway tunnel [10]. Although not shown herein, trial analyses were carried out to determine the size of the analyzed domain and the thickness of the finite elements in the vertical direction.

2.4. Input earthquake motion

The west-eastern component of the 1995 Kobe Earthquake was scaled and used as the horizontal excitation in the analyses, as shown in Fig. 3. No vertical excitation was used in the present study. The earthquake excitation was input at the base of the finite element domain. Different magnitudes of earthquake excitation were analyzed, i.e., the west-eastern component of the 1995 Kobe Earthquake was scaled to 0.08 g, 0.2 g, 0.3 g, 0.4 g, 0.5 g, 0.6 g and 0.8 g, respectively, in order to investigate the mechanism of uplift and the working mechanism of cutoff walls. The length of the excitation was truncated as 30 s. However, for some cases consolidation analyses were conducted after earthquake excitation for about 21 min. Ten-second-long sinusoidal waves of different magnitudes with a

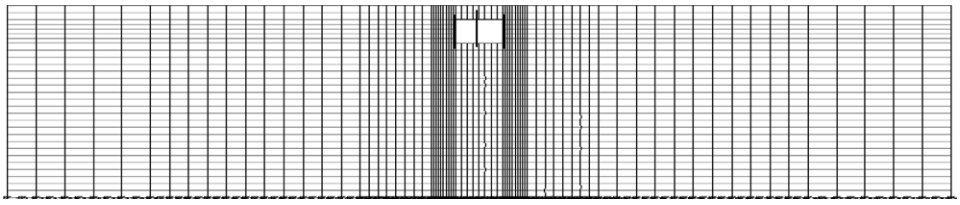

Fig. 2. Finite element mesh.

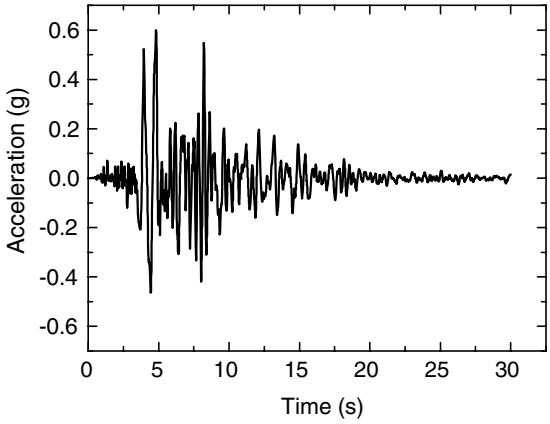

Fig. 3. Input earthquake excitation ($a_{max} = 0.6$ g).

frequency of 2 Hz were also used in order to investigate the lateral pressures acting on the cutoff walls.

The analysis procedure, the numerical integration scheme and the time step during the dynamic analyses were similar to those in the former investigation [10]. The initial stress states before earthquake excitation were assumed to be the same for the cases with and without cutoff walls, i.e., the installation or construction of cutoff walls did not disturb the stress states underneath the subway tunnel and in the far fields, which is similar to real situations. For the consolidation analyses, the time step for the first 30 seconds was still 0.005 s, and was changed to 0.05 s afterwards. Altogether more than 30 different cases were studied, with different magnitudes of earthquake excitation, without or with cutoff walls, and with different thickness, moduli, locations or permeabilities of cutoff walls. The cases with 0.6 g excitation input, without or with grouted cutoff walls (1.5-meter-thick and 0.0 m away from the subway tunnel with $E = 400$ MPa), were used as base cases. The parameters of the base cases were used throughout the analyses, with one of them varied to investigate the corresponding influences.

3. Mechanism of uplift and working mechanism of cutoff walls

3.1. The effects of cutoff walls

The effects of cutoff wall installation in alleviating the uplift of underground structures due to earthquake induced liquefaction were very obvious according to the finite element analysis results. As shown in Fig. 4, the uplift of the subway tunnel reduced very considerably under 0.6 g earthquake excitation if cutoff walls were installed. Figs. 5a and b show the comparison of deformed meshes after 30 seconds of shaking for the cases without and with cutoff walls. Clearly, the surrounding soils during earthquake were "squeezed" underneath the subway tunnel and "pushed" the underground structure up. The cutoff walls could reduce or even prevent such deformation and therefore the uplift of the subway tunnel in that case was much smaller. Fig. 5c shows the movement of a soil particle 1.5 m under the right corner of the subway tunnel. The squeezing of soils and the effects of cutoff walls in reducing such squeezing can be clearly seen from the figure.

The consolidation responses of the soil–structure interaction system are shown in Fig. 6. It could be seen in Fig. 6a that the underground structure settled during soil consolidation. However, the settlement was much smaller than the uplift due to soil liquefaction for the case without cutoff walls. Residual displacement of the subway tunnel existed after soil consolidation, indicating the squeezing of soil underneath it during earthquake loading. For the case with cutoff walls, the settlement after earthquake was larger than the uplift, leading to some net settlement of about 1.2 cm. The dissipation of excess pore pressure with cutoff walls was slower, as shown in Fig. 6b, due to the existence of cutoff walls that hindered the dissipation of excess pore pressure laterally. Observing the differences in the maximum and residual displacements, it can be seen that the existence of cutoff walls also reduced the settlement

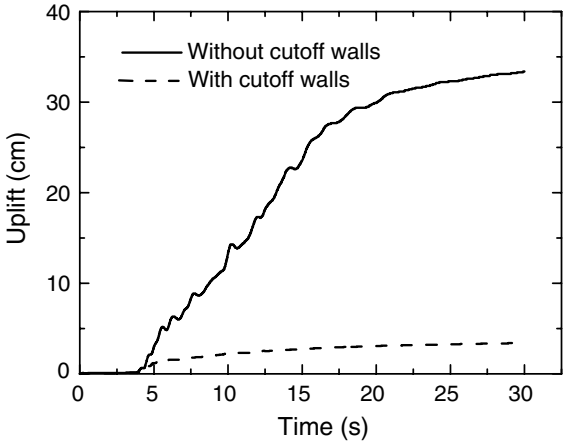

Fig. 4. Effects of cutoff walls in alleviating uplift.

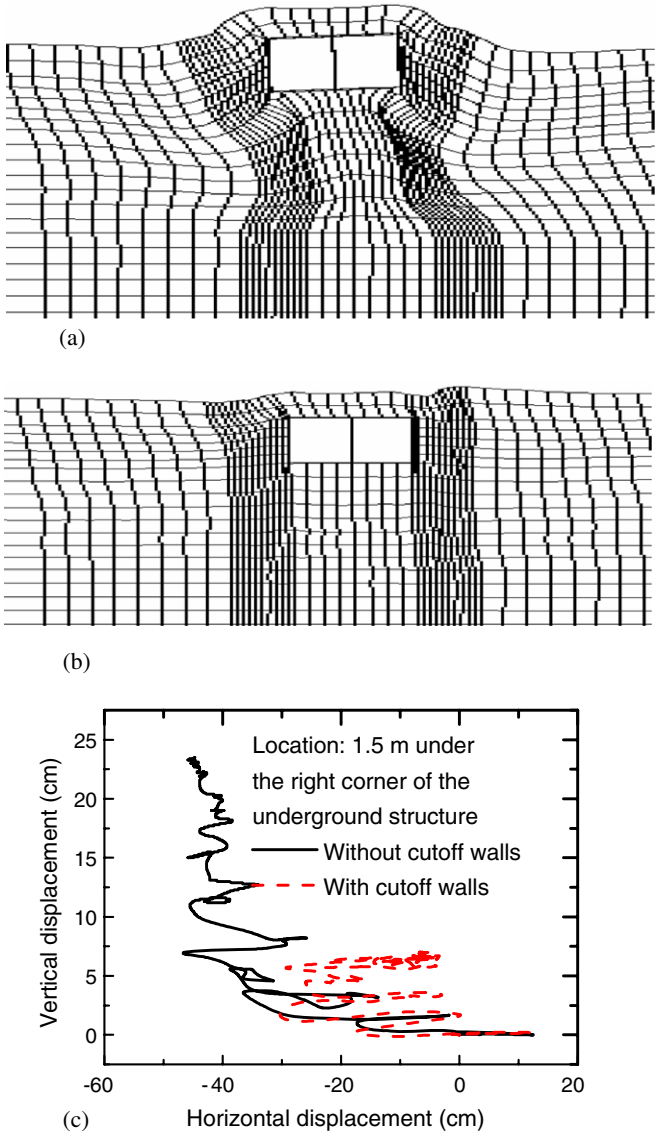

Fig. 5. Effects of cutoff walls in reducing the "squeezing" of soils. (a) Without cutoff walls, deformation enlarged 10 times. (b) With cutoff walls, deformation enlarged 10 times. (c) The movement of a soil particle 1.5 m under the right corner of the subway tunnel.

during soil consolidation, which is consistent with the findings by other investigators (e.g. [17]).

3.2. The effects of cutoff walls under different magnitudes of earthquake excitation

It is clear now that the installation of cutoff walls could reduce the "squeezing" of the surrounding soils underneath the subway tunnel and hence alleviate the uplift. But can the cutoff walls inhibit the development of excess pore pressure and prevent total liquefaction of the soils surrounding the subway tunnel? Different magnitudes of earthquake excitation were used to analyze the cases without and with cutoff walls (1.5-metre-thick and 0.0 m away from the subway tunnel with $E = 400$ MPa) to answer this question. Fig. 7 shows the developments of excess pore pressure at the location 3 m right below the subway tunnel. Clearly, under small amplitude of earthquake excitation, the cutoff walls could inhibit the build-up of excess pore pressure. However, under large earthquake excitations, the excess pore pressure in the case with cutoff walls was even larger than that in the case without cutoff walls.

The stress–strain relationships and the stress paths at the same location are given in Figs. 8 and 9, respectively. It can be seen that the cutoff walls could reduce the magnitude of shear deformation but the minimum mean effective pressure p' was even smaller in the cases with cutoff walls under large earthquake excitations. The reason lies in the fact that, first of all, the excess pore pressure in the case with cutoff walls was even larger; and secondly, the lateral effective stress was found to be larger than the vertical one for the case without cutoff walls during earthquake excitation due to the "squeezing" of soils underneath the subway tunnel.

It is also interesting to note that the effects of cutoff walls increase with an increase in the magnitude of earthquake excitation, as shown in Fig. 10. The uplift ratios were obtained by dividing the uplifts with cutoff walls by those without cutoff walls.

3.3. The mechanisms

The mechanism of uplift of underground structures in liquefiable soil during earthquake is now clear. The development of excess pore pressure led to a rapid decrease in the stiffness of the surrounding soil. The small effective unit weight made the underground structure be prone to uplift due to the differences in the total vertical pressure acting on it. The deformation or "flow" of the surrounding soil due to its small stiffness led to the "squeezing" of soil underneath the underground structure and "push it further up". The deformed mesh in Fig. 5a and the soil particle movement in Fig. 5c both indicate this mechanism. The finite element analysis results are in consistent with the analysis of uplift mechanism in Schmidt and Hashash [12].

The working mechanism of cutoff walls can also be explained based on the finite element analysis results. It could be seen in Fig. 7 that cutoff walls could not always inhibit the development of excess pore pressure underneath the underground structure. Cutoff walls could reduce the shear deformation in the soil, as indicated in Fig. 8. And under small earthquake excitation, the smaller shear deformation would lead to lower excess pore pressure. However, at relatively large shear deformation, the loose Nevada sand used in the analysis would dilate, as can be seen in the experimental results in Arulmoli et al. [26], which is also the property of most sandy soils at medium loose condition. The relatively small shear deformation amplitudes in the cases with cutoff walls were therefore not necessarily preferable in inhibiting the development of excess pore pressure. Observing the excess pore pressures in Fig. 7,

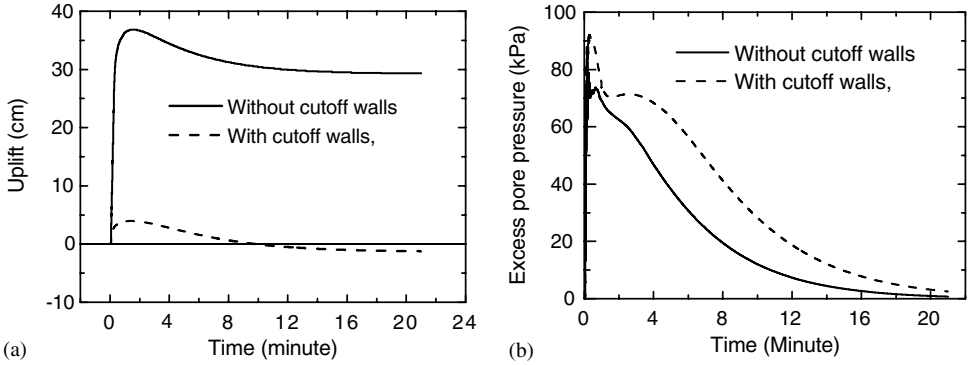

Fig. 6. Consolidation responses of the soil–structure interaction system: (a) vertical displacement of the subway tunnel, (b) dissipation of excess pore pressure.

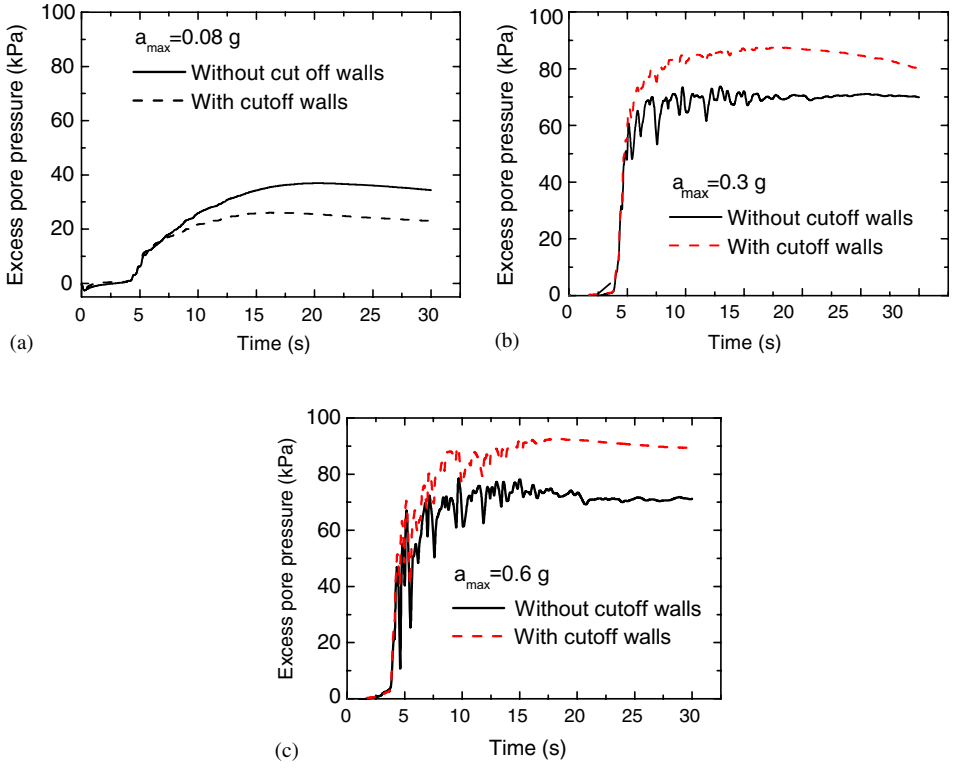

Fig. 7. The development of excess pore pressure under different magnitudes of earthquake excitations: (a) $a_{max} = 0.08$ g, (b) $a_{max} = 0.3$ g, (c) $a_{max} = 0.6$ g.

the stress–strain relationships in Fig. 8, and the stress paths in Fig. 9, it could be seen that the large cyclic shear deformations in the cases without cutoff walls could lead to the liquefaction of saturated sandy soils due to the large volume contraction tendency upon unloading [29], while for the cases with cutoff walls, although the volume contraction tendency upon unloading might be smaller due to the smaller shear deformation amplitudes, the soil tended to contract upon loading, in contract to the cases without cutoff walls. The transmission of earthquake energy by cutoff walls when the soil liquefies may also contribute to the higher excess pore pressure in the case with cutoff walls. The soil could also liquefy with cutoff walls installed, and the speed and magnitude of excess pore pressure development were even larger for the cases with large earthquake excitation, as shown in Fig. 7.

The paradox between Zheng et al. [16] and Adalier et al. [17] could now be explained. The soil and its density used in the centrifuge shaking table tests in Adalier et al. [17] were similar to the ones used in the present study. And with relatively large input excitation (up to 0.3 g sinusoidal wave), the excess pore pressure development in the case with cutoff walls would not be smaller than in the case without cutoff walls. While in Zheng et al. [16], the experienced

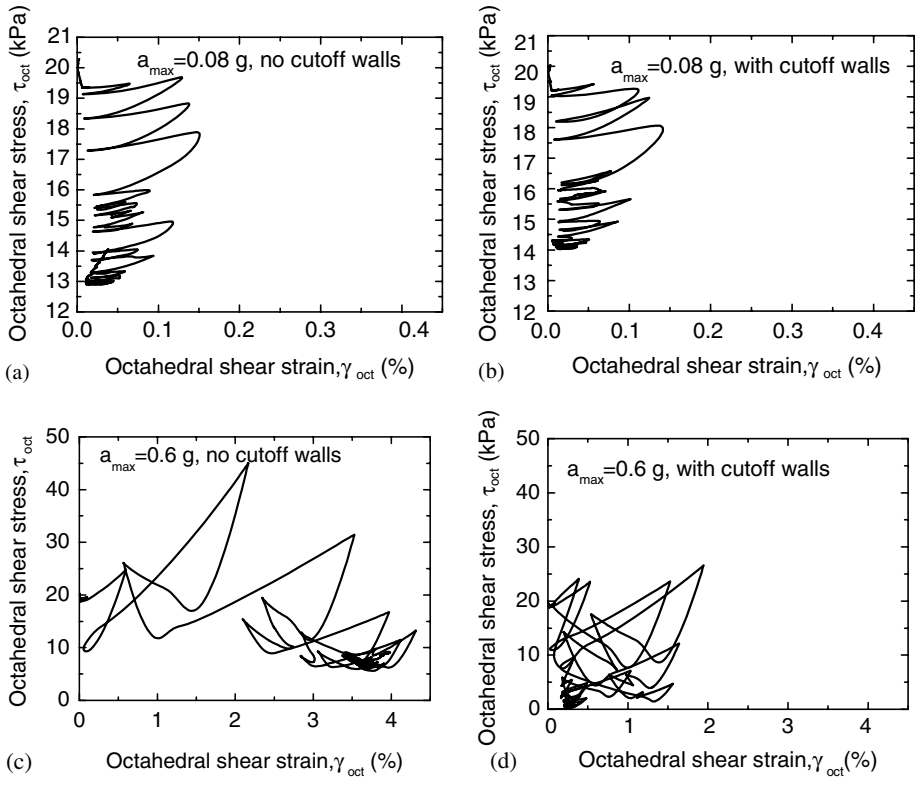

Fig. 8. Stress–strain relationships: (a) $a_{max} = 0.08$ g, without cutoff walls, (b) $a_{max} = 0.08$ g, with cutoff walls, (c) $a_{max} = 0.6$ g, without cutoff walls, (d) $a_{max} = 0.6$ g, with cutoff walls.

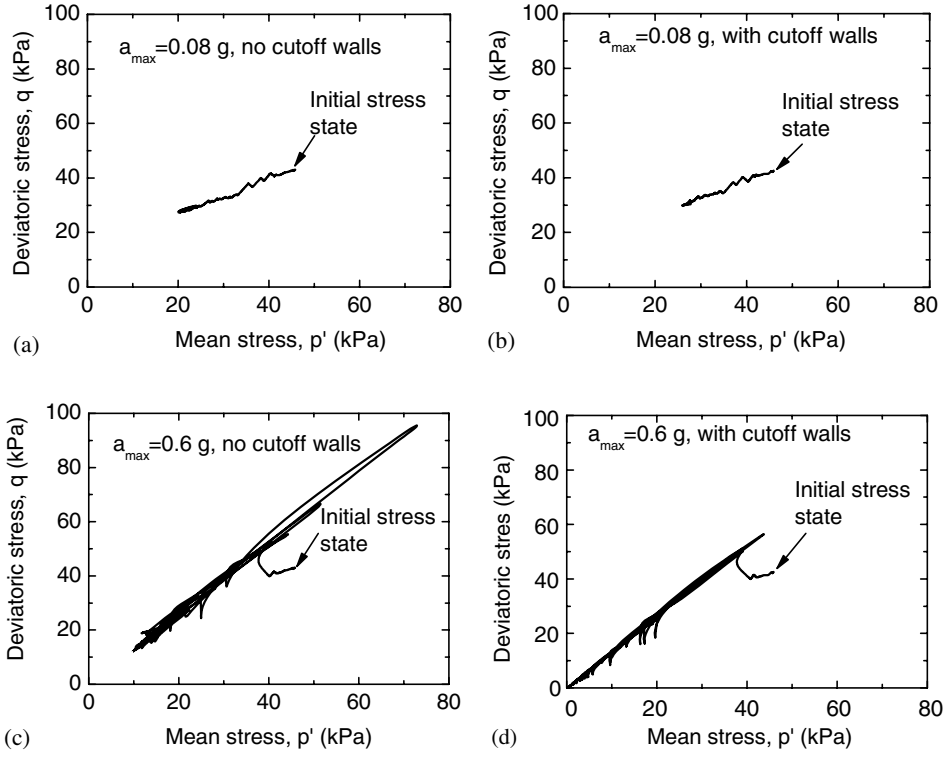

Fig. 9. Stress paths: (a) $a_{max} = 0.08$ g, without cutoff walls, (b) $a_{max} = 0.08$ g, with cutoff walls, (c) $a_{max} = 0.6$ g, without cutoff walls, (d) $a_{max} = 0.6$ g, with cutoff walls.

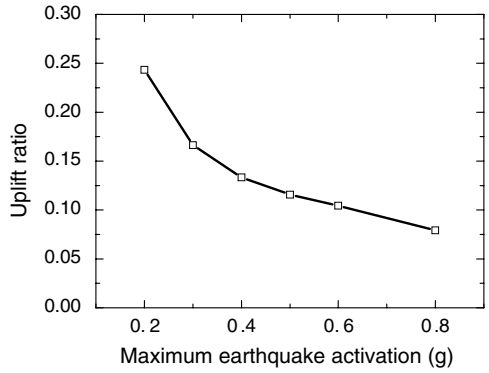

Fig. 10. Effects of cutoff walls under different magnitudes of earthquake excitations.

earthquake in the investigated location was rather small ($a_{max} = 0.16$ g), the excess pore pressure was then smaller in the case with cutoff walls due to the very small shear deformation. The situation may be different with very loose sand, as in the case in Ninomiya et al. [14]. Very loose sand would contract even at large shear deformation, which explains the smaller excess pore pressure in Ninomiya et al. [14] with cutoff walls installed. However, as indicated above, for most medium loose sand, which is more relevant in most cases, the phenomena found in this study would be more possible to occur.

In summary, cutoff walls could reduce the shear deformation of liquefiable soil subjected to earthquake excitation; however, whether they could inhibit the development of excess pore pressure depends on three factors: (1) the soil type; (2) the relative density of the soil; and (3) the magnitude of earthquake excitation. It would not be accurate to state that whether cutoff walls could or could not inhibit excess pore pressure development without referring to these three factors. Nevertheless, cutoff walls could restrain the deformation of liquefiable soil and hence reduce the damage due to soil liquefaction, e.g., the uplift of underground structures.

4. Design parameters of cutoff walls

The effectiveness of cutoff walls in alleviating the uplift of underground structures due to earthquake induced liquefaction has been demonstrated. Based on the working mechanism as discussed in last section, the design parameters for cutoff walls could also be analyzed, including the pressures acting on the cutoff walls, the locations, the modulus, the thickness, and the coefficient of permeability of cutoff walls. Only the lateral positions of cutoff walls were discussed, since it could be easily understood that cutoff walls must be penetrated into the non-liquefiable soil layer to certain length and enclose the liquefiable soil underneath underground structures to be effective.

4.1. The pressures acting on the cutoff walls during earthquake

The total lateral pressures acting on the cutoff walls were investigated with different magnitudes of Kobe earthquake excitations, ranging from 0.2 g to 0.8 g. In order to study the effects of earthquake characteristics, sinusoidal waves that lasted 10 seconds with a frequency of 2 Hz were also used, with a magnitude ranging from 0.1 g to 0.4 g. The total lateral pressure includes the effective earth pressure and the pore water pressure.

The pressure envelopes acting on the outer and inner sides of the left cutoff wall (relative to the underground structure) are shown in Figs. 11a and b, respectively. It can be seen that the total lateral pressures increased with an increase in the excitation amplitudes. The frequency characteristics of earthquakes had small effects on the pressures. Under small earthquake excitations, the pressures closer to the ground surface increased significantly due to soil liquefaction while those at deeper depth increased only slightly, indicating that the soils there were not liquefied. Under large earthquake excitations, the slope of the lateral pressure on the outer side was the unit weight of the liquefied soils (19.2 kN/m^3), which was in consistent with Yoshimi [30], and that of the pressure on the inner side was also approximately the same, which was larger than the value used in Yoshimi's analysis [30]. It was assumed in his analysis that the overburden stress underneath the underground structure was smaller due to the small effective unit weight of the underground structure and was uniformly distributed at the same depth. However, from the finite element analysis results, the overburden stress was

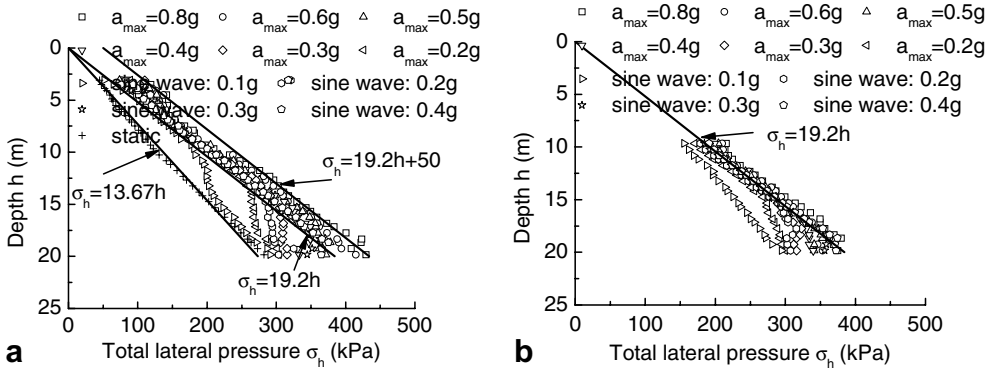

Fig. 11. Pressure envelopes acting on the outer and inner sides of the left cutoff wall: (a) outer (b) inner.

not uniform at the same depth below the underground structure and the one close to the side of the tunnel was almost the same as that in the far field of the tunnel, which explains the phenomenon shown in Fig. 11. However, the pressures on the outer side with large earthquake excitation were larger than the hydrostatic pressure of the liquefied soils, which might be due to the dynamic effect observed in the experiments by Tamari and Towhata [31].

It must be pointed out that the precise moments when the maximum pressure acting on the outer and inner sides, respectively, were not exactly the same, and that the pressures at those moments were slightly smaller than the envelopes at some locations, but the differences were very small. For design purpose, the pressure envelopes could be assumed as the maximum pressures and occur at the same time on the outer or inner side of the cutoff walls simultaneously. The pressure differences on the outer and inner sides of the left cutoff wall are shown in Figs. 12a and b for Kobe excitations $a_{max} = 0.8$ g and $a_{max} = 0.6$ g, respectively. The pressure difference for the case with larger earthquake excitation was larger as expected. The pressure differences might be explained by the so-called dynamic effects in Tamari and Towhata [31], since the accelerations of the soils surrounded by the cutoff walls were smaller. But the factors influencing the magnitude of the difference and its calculation must be further investigated, but it could be seen that the pressure difference was not large, even under large earthquake excitations. Nevertheless, the effects of lateral spreading due to earthquake induced liquefaction on the lateral pressure were not investigated in the present study. Things would certainly be different if there was lateral spreading.

4.2. The effects of lateral cutoff-wall locations

The effects of the lateral locations of cutoff walls on the uplift the underground structure are shown in Fig. 13. It could be seen that with an increase in the distance of the cutoff walls away from the subway tunnel, the uplift increased rapidly. This could simply be explained by the fact that although the cutoff walls prevented the flow of liquefied soils in the far field, the deformation of the liquefied soils between the cutoff walls and the subway tunnel still squeezed the underground structure to uplift. The results indicated that the construction or installation of cutoff walls must be as close to the protected underground structure as possible in order to be effective.

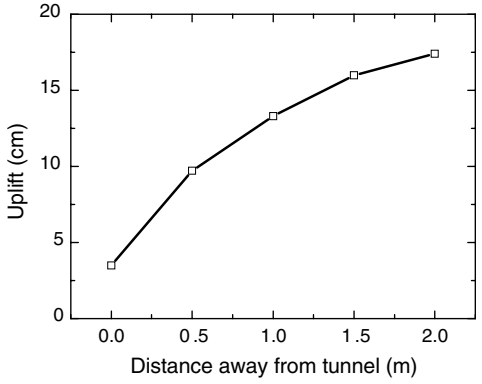

Fig. 13. Effects of the lateral locations of cutoff walls.

4.3. The effects of cutoff-wall modulus and thickness

The Young's modulus of the cutoff walls were varied from 100 MPa to 600 MPa to investigate the influences of cutoff-wall modulus, the results of which are shown in Fig. 14. It could be seen in Fig. 14a that the uplift of the underground structure reduced with an increase in the modulus. The higher stiffness of cutoff walls could better inhibit the deformation of liquefied soils, and as shown in Fig. 14b, the build-up of excess pore pressure was also smaller, indicating that higher stiffness could also restrain the excess pore pressure development. Similar to the effects of cutoff-wall modulus, the increase of cutoff-wall thickness would also reduce the tunnel uplift, as can be seen in Fig. 15a. Its influence on the excess pore pressure was also similar, as shown in Fig. 15b. The dependence of uplift on cutoff wall thickness was approximately linear.

4.4. The effects of cutoff-wall permeability

The effects of cutoff-wall permeability were finally analyzed and are given in Fig. 16. Similar to the experimental findings in Tanaka et al. [11], the drainage paths provided

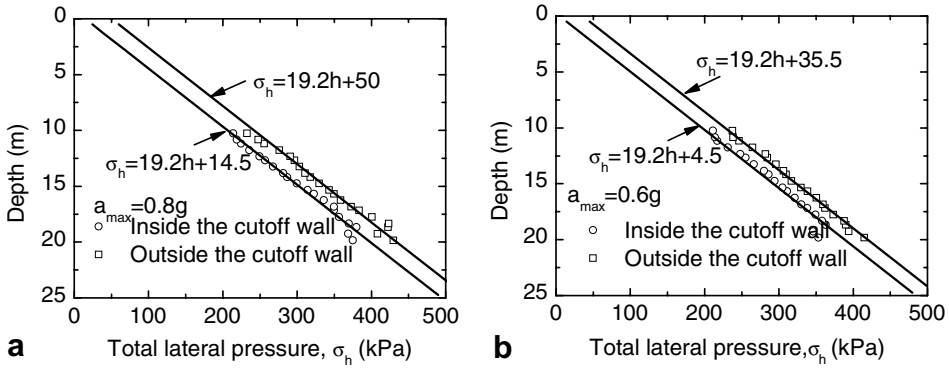

Fig. 12. Pressure differences on the outer and inner sides of the left cutoff walls.

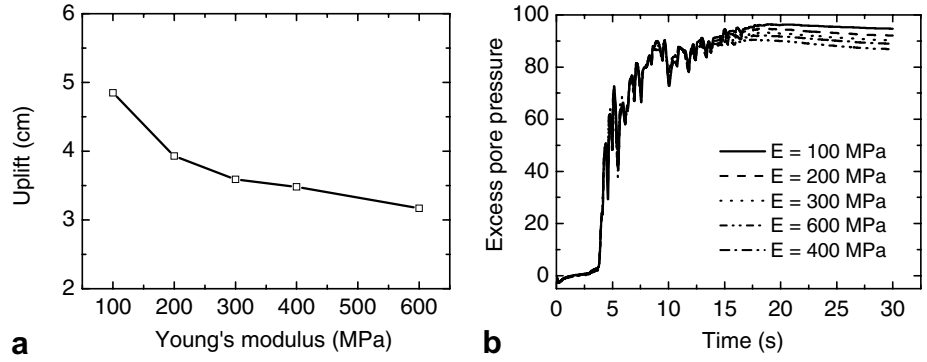

Fig. 14. Influences of cutoff-wall modulus: (a) uplift, (b) excess pore pressure at the location 3 m right below the subway tunnel.

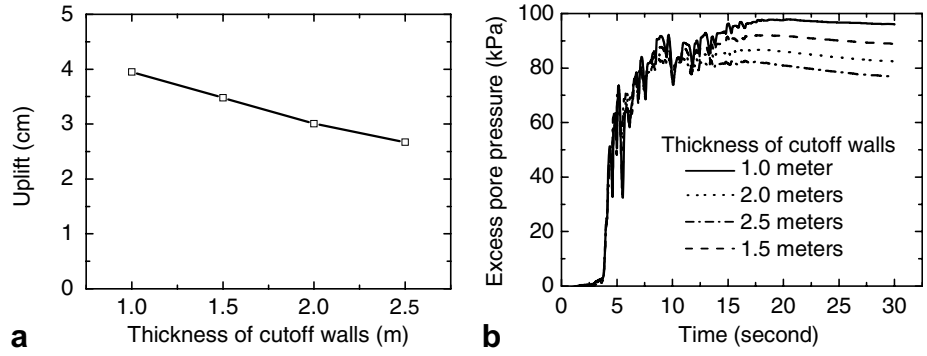

Fig. 15. Effects of cutoff-wall thickness: (a) uplift, (b) excess pore pressure at the location 3 m right below the subway tunnel.

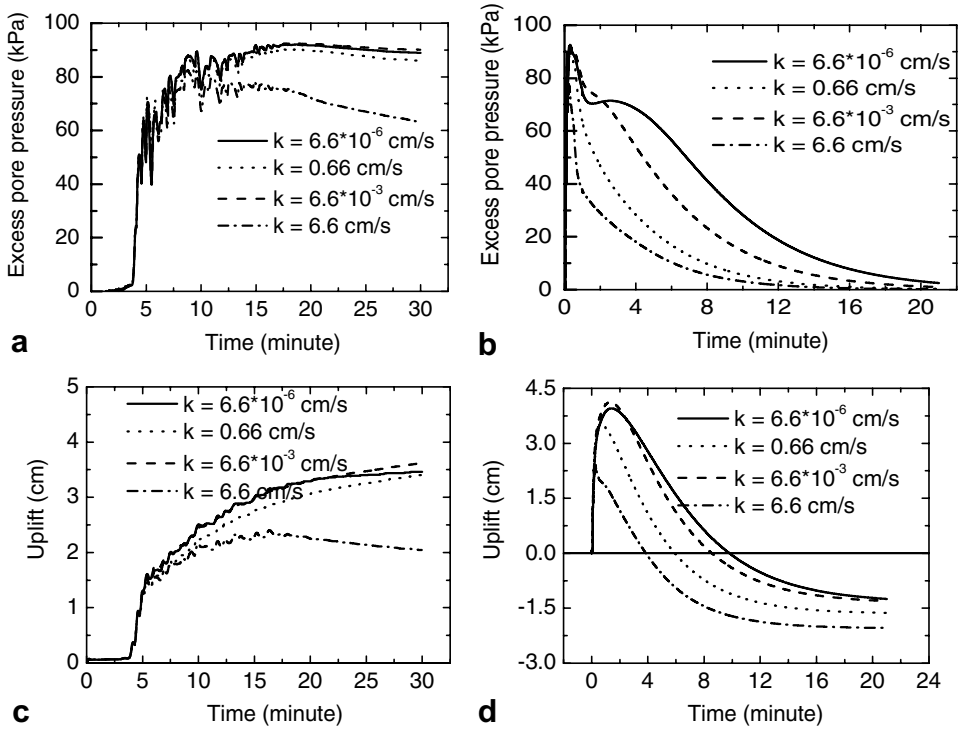

Fig. 16. Effects of cutoff-wall permeability: (a) excess pore pressure during earthquake, (b) excess pore pressure dissipation during consolidation, (c) uplift during earthquake, (d) uplift during consolidation.

by the cutoff walls could restrain the build-up of excess pore pressure and accelerate its dissipation after earthquake loadings, as shown in Figs. 16a and b. Accordingly, the uplift of the subway tunnel was smaller with larger coefficient of permeability, as shown in Figs. 16c and d, but the amount of final settlement was larger, as can be seen in Fig. 16d. Surely, the coefficient of permeability must be large enough to be effective. In the analyses, the uplift for the case with $k = 6.6 \times 10^{-3}$ cm/s was even slightly larger than that for the case with $k = 6.6 \times 10^{-6}$ cm/s, which might be due to some numerical issues. It would also be interesting to compare the net displacements of the subway tunnel, which was obtained by subtracting the displacements at the end of consolidation from the maximum uplifts. For the base case, the net displacement was 5.2 cm, while for the case with $k = 6.6$ cm/s, it was about 4.4 cm. The net displacement of the subway tunnel was smaller with additional drainage paths provided by the cutoff walls.

5. Conclusions and discussions

The uplift mechanism of underground structures in liquefiable soils under strong earthquake excitations and the working mechanism of cutoff walls in alleviating the uplift were analyzed using fully coupled finite element method. The liquefiable soil was simulated using a generalized plasticity model that had been proved to be able to reproduce the salient features of sandy soils including pressure dependency, cyclic liquefaction and cyclic hardening. The lateral pressures acting on the cutoff walls during earthquake excitations, the influences of cutoff-wall location, modulus, thickness, and permeability were analyzed to examine the various design parameters necessary for cutoff wall design. The consolidation responses of the soil–structure system after earthquake excitation were also investigated. From the numerical analyses, the following conclusions can be obtained:

(1) The uplift of underground structures in saturated liquefiable soils during strong earthquakes can be explained by three factors: the small effective unit weight of underground structures, the development of excess pressure and the flow of liquefied soils towards the underneath of underground structures. The small effective unit weight of underground structures and the excess pressure build-up only establish the necessary conditions of uplift. Uplift can be inhibited if the flow or deformation of liquefied soils is prevented.
(2) Installation of cutoff walls next to underground structures and sufficiently penetrated into the underlying non-liquefiable soil can restrict the liquefaction induced uplift. Cutoff walls prevent the flow or deformation of liquefied soil from squeezing the underground structure to uplift, and they reduce the shear deformation in the enclosed soils, but it cannot always inhibit the development of excess pressure. In comparison with the case without cutoff walls, the magnitude of excess pore pressure of the enclosed liquefiable soils may be larger or smaller, depending on the soil properties and earthquake excitation magnitude.
(3) Underground structures may settle during the consolidation process after earthquakes and the existence of cutoff walls can reduce such settlement. However, if the uplift during earthquake loading is large due to flow of liquefied soils, the magnitude of settlement is smaller than the uplift; while for the cases with cutoff walls, the magnitude of settlement may be larger.
(4) The lateral pressures acting on the outer and inner sides of cutoff walls may both be approximated using straight lines with the total unit weight of the adjacent liquefiable soils as slopes if the soils are sufficiently liquefied in strong earthquakes. However, the pressure on the outer side is larger due to the stronger dynamic effect.
(5) Cutoff walls must be constructed as close as possible to underground structures to be effective. Their stiffness, either in modulus or in thickness, is critical and must be large enough. And the drainage paths provided by cutoff walls with large coefficient of permeability can accelerate the dissipation of excess pore pressure and reduce the uplift of underground structure.

Although cutoff walls can restrain the uplift of underground structures during earthquake loadings and the corresponding settlement afterwards, they are not able to inhibited the development of excess pore pressure in many cases and totally eliminate the vertical displacement of underground structures. Therefore, the method usually must be combined with other measures, both structurally and geotechnically, such as stronger reinforcements in the underground structures, soil densification, gravel drainage, and so on. And in order to establish a rational design method for cutoff walls, the net lateral pressure acting on them must be further investigated.

Acknowledgements

The study was carried out under the supports of the Natural Science Foundation of China (Grant No. 50378050) and the Ministry of Education of China (under a fund for returned oversea students). The two supports are gratefully acknowledged. The authors are also appreciative to Dr. Andrew H.C. Chan of the University of Birmingham for the allowance of using the DIANA Swandyne-II program for the study. The authors are thankful to the reviewers of the paper for their insightful comments.

References

[1] Hall WJ, O'Rourke TD. Seismic behaviour and vulnerability of pipelines. Lifeline earthquake engineering. New York: ASCE; 1991. p. 761–73.

[2] O'Rourke TD, Gowdy TE, Stewart HE, Pease JW. Lifeline and geotechnical aspects of the 1989 Loma Prieta Earthquake. In: Proceedings of the 2nd international conference on recent advances in geotechnical earthquake engineering and soil dynamics. Rolla (MO): University of Missouri-Rolla; 1991. p. 1601–12.
[3] Mohri Y, Yasunaka M, Shigeru T. Damage to buried pipeline due to liquefaction induced performance at the ground by the Hokkaido–Nansei–Oki earthquake in 1993. In: Proceedings of the 1st international conference on earthquake geotechnical engineering. Rotterdam, The Netherlands: Balkema; 1995. p. 31–6.
[4] Sasaki T, Koseki J, Matsuo O, Saito K, Yamashita M. Analyses of damage to sewer pipes in Shibetsu Town during the 1994 Hokkaido–Toho–Oki earthquake. In: Proceedings of the 1999 5th US conference on lifeline earthquake engineering: optimazing post-earthquake lifeline system reliability, Seattle (WA), USA; 1991. p. 247–56.
[5] Shinozuka M, Ballantyne D, Borcherdt R, Buckle I, O'Rourke TD, Schiff A. The Hanshin–Awaji earthquake of January 17, 1995. Performance of lifelines. Technical Report Prepared for NCEER, Buffalo (NY); 1995.
[6] Tsai J, Jou L, Lin SH. Damage to buried water supply pipelines in the Chi–Chi (Taiwan) earthquake and a preliminary evaluation of seismic resistance of pipe joints. J Chin Inst Eng, Trans Chin Inst Eng 2000;23(4):395–408.
[7] Schmidt B, Hashash YST. US immersed tube retrofit. Tunnels Tunneling Int 1998;30(11):22–4.
[8] Taylor PR, Ibrahim HH, Yang D. Seismic retrofit of George Massey Tunnel. Earthquake Eng Struct Dyn 2005;34:519–42.
[9] Orense RP, Morimoto I, Yamamoto Y, Yumiyama T, Yamamoto H, Sugawara K. Study on wall-type gravel drains as liquefaction countermeasure for underground structures. Soil Dyn Earthquake Eng 2003;23(1):19–39.
[10] Liu H, Song E. Seismic response of large underground structures in liquefiable soils subjected to horizontal and vertical earthquake excitations. Comput Geotech 2005;32(4):223–44.
[11] Tanaka H, Kita H, Iida T, Saimura Y. Countermeasure against liquefaction for buried structures using sheet pile with drain capacity. Earthquake geotechnical engineering. Rotterdam, The Netherlands: Balkema; 1995. p. 999–1004.
[12] Schmidt BS, Hashash YMA. Preventing tunnel floatation due to liquefaction. In: Proceedings of the 2nd international conference on earthquake geotechnical engineering, Lisbon, Portugal; 1999. p. 509–12.
[13] Hashash YMA, Hook JJ, Schmidt B, Yao J. Seismic design and analysis of underground structures. Tunnelling Underground Space Technol 2001;16(4):247–93.
[14] Ninomiya Y, Hagiwara R, Azuma T. Rise of excess pore water pressure and uplift of underground structures due to liquefaction. Earthquake geotechnical engineering. Rotterdam, The Netherlands: Balkema; 1995. p. 1023–28.
[15] Koseki J, Matsuo O, Koga Y. Uplift behaviour of underground structures caused by liquefaction of surrounding soil during earthquake. Soils Foundations 1997;37(1):97–108.
[16] Zheng J, Suzuki K, Ohbo N, Prevost J. Evaluation of sheet pile ring countermeasure against liquefaction for oil tank site. Soil Dyn Earthquake Eng 1996;15:369–79.
[17] Adalier K, Elgamal A, Martin G. Foundation liquefaction counter measures for earth embankments. J Geotech Geoenviron Eng, ASCE 1998;124(6):500–17.
[18] Khoshnoudian F, Shahrour L. Numerical analysis of the seismic behaviour of tunnels constructed in liquefiable soils. Soils Foundations 2002;42(6):1–8.
[19] Yang D, Naesgaard E, Byrne PM, Adalier K, Abdoun T. Numerical model verification and calibration of George Massey Tunnel using centrifuge models. Can Geotech J 2004;41:921–42.
[20] Chan AHC. User manual for DIANA SWANDYNE-II. UK: School of Civil Engineering, University of Birmingham; 1993.
[21] Madabhushi SPG, Zeng X. Seismic response of gravity quay wall. II: Numerical modeling. J Geotech Geoenviron Eng, ASCE 1998;24(5): 418–27.
[22] Aydingun O, Adalier K. Numerical analysis of seismically induced liquefaction in earth embankment foundations. Part I. Benchmark model. Can Geotech J 2003;40(4):753–65.
[23] Liu H, Ling HI. A sand model based on generalized plasticity. In: Constitutive modeling of geomaterials: selected contributions from Frank L. DiMaggio symposium. Boca Raton (FL): CRC Press; 2002. p. 40–6.
[24] Ling HI, Liu H. Pressure dependency and densification behaviour of sand through a generalized plasticity model. J Eng Mech, ASCE 2003;129(8):851–60.
[25] Liu H. Finite element simulation of the response of geosynthetic-reinforced soil walls. PhD thesis, Columbia University, New York; 2002.
[26] Arulmoli K, Muraleetharan KK, Hossai MM, Fruth LS. Verification of liquefaction analysis by centrifuge studies laboratory testing program soil data. Technical Report, Earth Technology Corporation, Irvine (CA), USA; 1993.
[27] Arurlanandan K, Scott RF. Verification of numerical procedures for the analysis of soil liquefaction problems. Rotterdam, The Netherlands: Balkema; 1993.
[28] Yang S, Ling HI. Calibration of a generalized plasticity model and its application to liquefaction analysis. In: Soil constitutive models: evaluation, selection and calibration, ASCE geotechnical special publication 128; 2005. p. 483–94.
[29] Pastor M, Zienkiewicz OC, Chan AHC. Generalized plasticity and the modeling of soil behaviour. Int J Numer Anal Meth Geomech 1990;14(3):151–90.
[30] Yoshimi Y. Simplified design of structures buried in liquefiable soil. Soils Foundations 1998;38(1):235–40.
[31] Tamari Y, Towhata I. Seismic soil–structure interaction of cross sections of flexible underground structures subjected to soil liquefaction. Soils Foundations 2003;43(2):1–8.